Original Article

Production of recombinant chimeric swine PKR-APAF-1 protein and its apoptotic induction on MARC-145 cells

Phong Vu Anh Tuan Vo[1] Thanaporn Leksakchai[1] Roongtham Kedkovid[1]

Achara Tawatsin[1] Athipoo Nuntaprasert[1*]

Abstract

Porcine reproductive and respiratory syndrome (PRRS) is one of the most important diseases of swine that has adverse effects on the pig industry as a result of direct and indirect loss (Li *et al*. 2007). Many methods have been applied to control this important viral disease in swine farms, however outbreaks are still taken place. The use of recombinant chimeric swine PKR-Apaf-1 protein (rcPAP) generated from human Double-stranded RNA (dsRNA) Activated Caspase Oligomerizer (DRACO) concept is an alternative way to control swine viruses. This rcPAP consisted of the Human Immunodeficiency Virus Trans-activator transcription (HIV-TAT) domain, the dsRNA-binding domain of porcine Protein kinase R (PKR) gene and the caspase recruitment domain (CARD) of the porcine Apoptotic Protease-Activating Factor-1 (Apaf-1) gene. This study aimed to produce rcPAP using a bacterial expression system and investigate its biological activity. Recombinant vectors pET-P-A and pQE32-P-A were constructed. The His-tag fusion proteins were expressed in *E. coli* and purified under native condition with the HiTrap chelating affinity column. The soluble rcPAP produced from the pET-P-A plasmid with a yield of 12.32 mg per liter of bacterial culture media at 25 °C for 18 h were 2.4-fold higher than the pQE32-P-A plasmid and were selected for *in vitro* study. The purified protein reacted with the mouse_anti-rcPAP polyclonal antibodies. The rcPAP (80 µg/mL) induced apoptosis in PRRS virus-infected MARC-145 cells at 48 hpi by increasing the monkey active caspase-3 value by 17.9 fold was higher (9.150 ± 0.008 vs 0.510 ± 0.003 ng/mg protein) when compared to uninfected control. The bioactivity *in vitro* indicates this established protein as a prospective molecule for research to control of PRRS virus infection.

Keywords: Bacterial expression, Purification, Protein, PKR, Apaf-1

[1]*Faculty of Veterinary Science, Chulalongkorn University, Henri-Dunant Rd., Pathumwan, Bangkok 10330, Thailand*
****Correspondence**: Athipoo.N@chula.ac.th* (A. Nuntaprasert)

Introduction

Swine farms today have encountered a real battle in multiple and complicated viral diseases. Porcine reproductive and respiratory syndrome (PRRS) is one of the most important diseases of swine having adverse effects on the pig industry as a result of direct and indirect loss (Li *et al*., 2007). Swine farms today have encountered a real battle with multiple and complicated viral diseases. Porcine reproductive and respiratory syndrome (PRRS) is one of the most important diseases of swine making adverse effects on pig industry as a result of direct and indirect losses (Le *et al*. 2019), etc. Swine farms today have encountered a real battle on the multiple and complicated viral diseases. Porcine reproductive and respiratory syndrome (PRRS) is one of the most important diseases of swine making adverse effects on pig industry as a result of direct and indirect losses (Charerntantanakul 2012). Antiviral therapeutics is a critical tool for combatting viral infections. Recently, Gao *et al*., (Gao *et al*. 2013) showed that *Cryptoporus volvatus* extract exhibited antiviral activity against PRRSV infection and replication. In 2015, lithium chloride could inhibit PRRSV replication (Cui *et al*., 2015). Moreover, the use of antiviral inhibitory drugs on the control of swine viral diseases has been limited in comparison with the use of antimicrobial agents (Pozzo and Thiry 2014).

In 2011, human Double-stranded RNA (dsRNA) Activated Caspase Oligomerizer (DRACO) proteins were developed and were effective against a broad spectrum of viruses such as Flaviviruses, Bunyaviruses and the Influenza virus (Rider *et al*., 2011). The human DRACO detects the long dsRNA helices of many viruses during transcription and replication and also induces rapid apoptosis selectively in virus-infected cells while leaving uninfected cells unharmed. However, there is little information to have reported the use of recombinant protein to reduce viral circulation in veterinary medicine (Pozzo and Thiry 2014). In 2015, Guo *et al*., reported the use of DRACO in pigs (Guo *et al*., 2015). This DRACO was synthesized based on the sequence of two natural cellular pathways and was constructed using porcine PKR and human Apaf-1 instead of porcine Apaf-1. The results showed that DRACO exhibits antiviral activity against highly pathogenic PRRS (HP-PRRS) virus infection in both MARC-145 cells and porcine alveolar macrophages (PAMs). The multiple alignments and similarity of deduced amino acid sequences (Table 1) of two dsRNA-binding domains of porcine PKR and CARD domain of porcine Apaf-1 gene had 58.2 % and 87.6 % of similarity to human PKR gene and Apaf-1 gene, respectively. These results revealed that two dsRNA-binding domains of human PKR and CARD domain of human Apaf-1 genes may not have a similar functional activity in pigs. The antiviral molecules such as human DRACO protein which originated from swine origin may play an important role as a self-defense mechanism for the control of viral infection in pigs. Therefore, we established an efficient cloning and expression system for soluble recombinant chimeric swine PKR-Apaf-1 proteins in *Escherichia coli*. In addition, the recombinant protein was purified via affinity chromatography and its bioactivity was assessed *in vitro*.

Table 1 Comparison homology (%) of deduced amino acid sequences of the dsRBD of porcine PKR and the CARD domain of porcine Apaf-1 gene with those of other mammalian species

Sequences	Cattle	Mouse	Human
dsRBD of porcine PKR	68.50%	50%	58.20%
CARD domain of porcine Apaf-1	92.70%	85.50%	87.60%

Materials and Methods

Bacterial strains, PRRS virus and plasmid vectors: The pCR2.1 TA plasmid (Invitrogen, USA), the pQE32 (QIAGEN, Germany) and pET-His6-TEV-LIC plasmids (Addgene, USA) were used to construct and express TAT-PKR-Apaf-1 protein and transformed into DH5α, M15 (pREP4) and BL21 (DE3) *E. coli* strains. The US strain PRRS virus (Thai isolated 01NP01 and stock virus at 6 log10 TCID50/ml) were used in this study. PRRS virus was propagated in MARC-145 cells.

Expression of recombinant chimeric swine PKR-APAF-1 protein (rcPAP):

Cloning: The purified PCR products encoding the dsRBD of porcine PKR (P) (GenBank Accession Number: AB104654) (Asano *et al*., 2004) and CARD domain of porcine Apaf-1 (A) (GenBank Accession Number: XM_003481742) (Riedl *et al*., 2005) cDNA from US strain PRRS virus-infected PAMs were directly inserted in pCR2.1®TA plasmid (Invitrogen, California, USA) using primers as shown in Table 2. The HIV-TAT domain was added into PKR forward primer (amino acid sequence: YGRKKRRQRRR) (Gump and Dowdy 2007). The plasmids were named pCR2.1-P and pCR2.1-A. The fragment was digested from pCR2.1-A and inserted into pCR2.1-P at the EcoRV restriction enzyme site. The correct orientation of the pCR2.1-P-A plasmids was confirmed by PCR technique, restriction enzymes and sequencing technique. The P-A fragments were amplified from the pCR2.1-P-A plasmids with specific primers (Table 2) and inserted into the pET-His6-TEV-LIC plasmid using the ligation-independent cloning (LIC) method (MacroLab 2014). Transformants (pET-P-A) (Fig. 1A) were screened for correct insertion. The P-A fragments were digested from the pCR2.1-P-A and inserted into the pQE32 plasmid at SmaI and SalI restriction enzyme sites. Transformants (pQE32-P-A) (Fig. 1B) were screened for correct insertion.

Expression of rcPAP and optimization of expression conditions: The positive transformant of each recombinant plasmid was propagated in 3 mL of LB media containing appreciate antibiotic at 37 ˚C with

rapid shaking at 200 rpm overnight. The pre-warmed medium (including antibiotics) was inoculated with overnight cultures and grown to an OD_{600} nm of about 0.6. The cultures were divided. Both fractions (induced with IPTG to a final concentration of 1 mM and non-induced as control) were grown for an additional 5 h with constant shaking. The cell pellets were re-suspended in SDS-PAGE loading buffer and were heated at 95 ˚C for 5 mins. A ten µL of each sample was loaded onto a 12.5 % SDS-PAGE gel and the gel was stained with Coomassie brilliant blue-R250 (CBB) (Bio Basic, Canada). The expression level of the rcPAP from two plasmids was studied at four temperatures (18, 25, 30 and 37 °C) using ImageJ image analysis software (http://imagej.nih.gov/ij) (Nguyen *et al*., 2014). To optimize expression conditions, three expression parameters, including IPTG (0, 0.1, 0.25, 0.5, 0.75, 1.0, and 2 mM) concentration, OD_{600} nm (0.5, 0.6, 0.7, 0.8, 1 and 1.2) value and induction time (0, 2, 4, 6, 8, 10, 12, and 18 h) were properly determined under optimized temperature.

Table 2 Nucleotide sequences of the primers used in this study

Gene	Sense	Sequence (5′ to 3′)	GenBank accession number	Product sizes (bp)	Reference
1. TAT-PKR RBD part	+	*CCCGGG*TATGGTCGTAA AAAGCGTCGTCAGCGTC GTCGTGCCAGTGGTCGT TCA	AB104654	576	12
	-	TCAGACTGTGCTTTTCA CAGA			
2. Apaf-1 CARD part	+	*GATATC*GATGCAAAAGC TCGAAATTGT	XM_003481742	291	10
	-	*GTCGAC*GGAAGAAGAG ACGACAGG			
3. TAT- RBD-PKR - CARD Apaf-1	+	TACTTCCAATCCAATGC ATATGGTCGTAAAAAGCGTC GTCAG	AB104654; XM_003481742	846	10, 12
	-	TTATCCACTTCCAATGT TATTAGGAAGAAGAGA CGACAGG			

❖ Restriction enzyme sites in the primers are underlined

❖ PRK forward primer including TAT HIV domain (33 bp)

The expression level was evaluated with ImageJ image analysis software (http://imagej.nih.gov/ij) (Nguyen *et al*. 2014). The SDS-PAGE gel bands measured the percentage of expressed recombinant proteins and these were compared to one another. The three-dimensional structure of the rcPAP was predicted from its amino acid sequences using I-TASSER software (http://zhanglab.ccmb.med.umich.edu/I-TASSER/) (Roy *et al*. 2010).

The solubility level of the rcPAP produced from the plasmids, *E. coli* pellets were obtained from 300 mL of cell cultures induced with IPTG, re-suspended in lysis buffer (BIO-RAD, USA) and then sonicated on ice for 10 min (Vo and Nuntaprasert 2015). After sonication, the cell suspensions were centrifuged at 12,000 rpm for 10 mins at 4 °C. The supernatant and pellet were collected and analyzed on 12.5 % SDS-PAGE. The solubility level measured the percentage of soluble and pellet fractions at the induction temperature with ImageJ image analysis software.

Purification of rcPAP: To prepare purified recombinant chimeric proteins, the M15 (pQE32-P-A) and BL21 (DE3) (pET-P-A) cell pellets were re-suspended in lysis buffer (BIO-RAD, USA) and incubated on ice for one hour. The suspension was sonicated on ice and centrifuged at 12,000 rpm at 4 ˚C for 30 mins. HiTrap chelating affinity column (HiTrap™ Chelating HP, Germany) was used to purify. The rcPAP were eluted with elution buffer in various concentrations of imidazole (0.1, 0.2, 0.3, 0.4, 0.5 and 1 M). The eluted proteins were analyzed in 12.5 % of SDS-PAGE and confirmed using western blot and dialyzed against PBS overnight using the Cellu-Sep® T2 Tubings dialysis membrane (Membrane Filtration Products, USA). The rcPAP concentration was measured upon the Bradford assay using the Bicinchoninic Acid (BCA) protein Assay Kit (Thermo Fisher Scientific, USA) with bovine serum albumin (BSA) that is standard under the manufactorer's instruction. Proteins were aliquot and were stored at -80 ˚C until further use.

Cytotoxicity assay: The cytotoxicity of rcPAP was evaluated using MTT assay on MARC-145 cells in six independent experiments. Each experiment involved triplicate wells per concentration. MACR-145 cells were detached using 0.5 % Trypsin/EDTA (Invitrogen, USA), re-suspended in complete medium and then dispensed into 96-well plates at a density of 10^3 cells per well. After 24 h of incubation, the rcPAP were administered to the wells at varying final concentrations (40, 60, 80, and 120 µg/mL) , followed by incubation for 48 h (Guo *et al*. 2015). Subsequently, 10 µL of MTT reagent (5 mg/mL) (Dojindo, Japan) was added to each well (Ding *et al*. 2005) and incubated for 4 h prior to the addition of 100 µL of 10 % (v/v) SDS in 50 % (v/v) N, N-dimethylformamide (Merck, USA) without removing the medium (Uma *et al*. 2008). An ELISA plate reader (Multiskan EX, USA) was used to record the absorbance at 570 nm. The percentage of cell viability was calculated using the following equation:

% Cell viability = 100 - % Cytotoxicity (% Cytotoxicity = 1- (mean absorbance of treated cells/ mean absorbance of negative control)) (Valiyari *et al*. 2012).

The cytotoxic effect of rcPAP on cell lines (as above) was also determined by the Trypan blue viability assay (Billack *et al*. 2008). Cells (10^4 per well) in 24 well-plates were cultured at varying-final concentrations of rcPAP (as shown above) for 48 h (Guo *et al*. 2015). Cells were detached by adding 100 µL of 0.5 % Trypsin/EDTA (Invitrogen, USA). DMEM supplement with 10 % FBS (50 µL) and 0.5 % Trypan blue (50 µL) (Merck, USA) were added to each well and the plates were incubated for 5 mins. Then, a 20 µL aliquot was removed and placed on a Neubauer hemocytometer (Precicolor, Germany). Finally, the numbers of viable and nonviable cells was counted under a microscope. The percent viability was calculated as: (viable cells/ the total cell count) × 100.

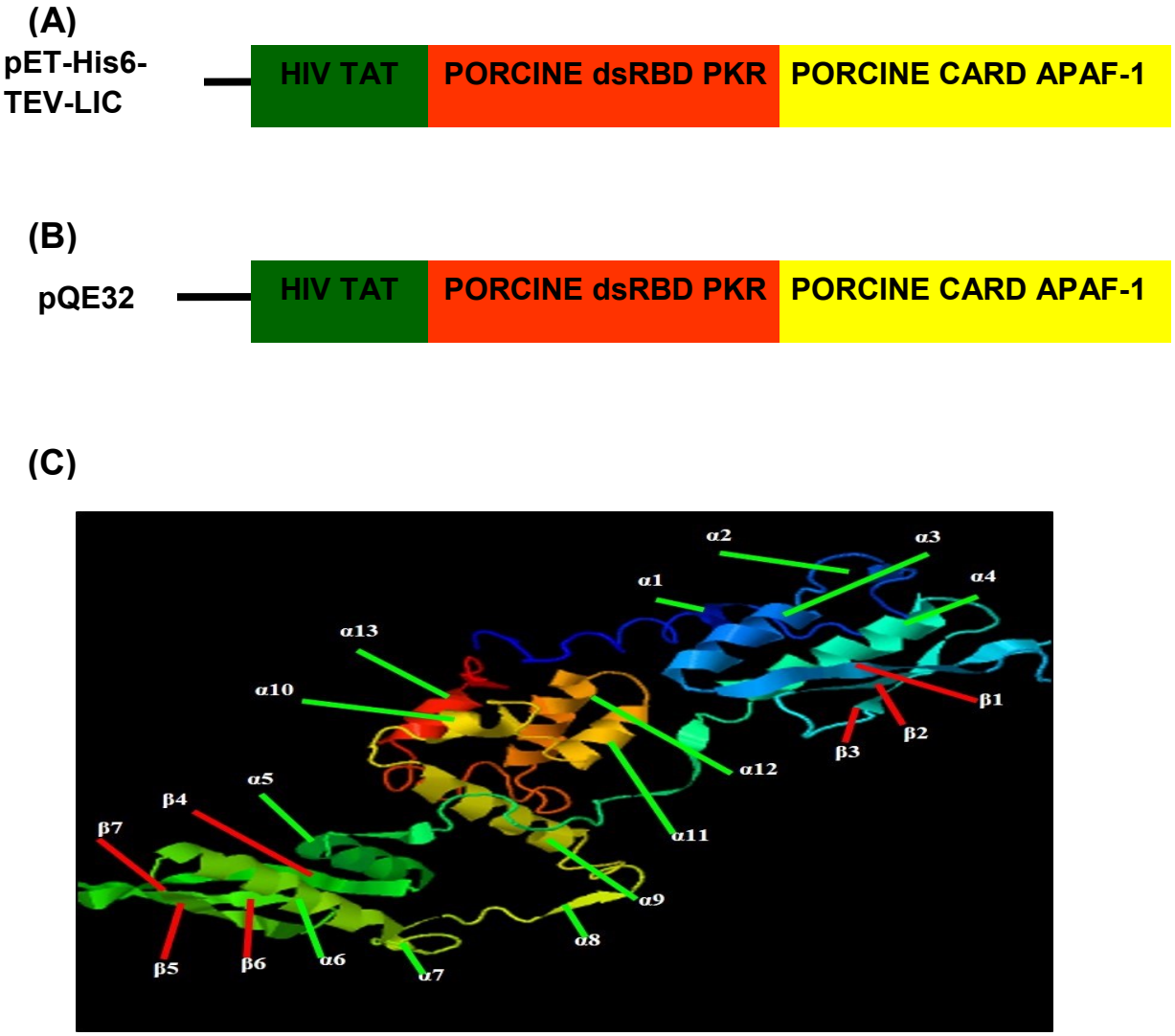

Figure 1 The recombinant chimeric PKR-Apaf-1 protein (rcPAP) construction and ribbon depiction. A) Schematic diagrams of rcPAP in pET-His6-TEV-LIC plasmid. B). Schematic diagrams of rcPAP in pQE32 plasmid. C)The I-TASSER model of the rcPAP (http://zhanglab.ccmb.med.umich.edu/I-TASSER/).

Apoptotic assay: The rcPAP were examined for their ability to induce apoptosis in PRRS virus-infected MARC-145 cells using Monkey Active caspase-3 ELISA Kit (MyBio-Source, USA) in 96-well plates under manufacturer's instructions. After 48 h treating cells with different concentration of the rcPAP at 0, 2, 5, 10, 20, 40, 80 and 160 µg/mL in the absence of viral infection or in the presence of high titer of PRRS virus (MOI=1) on MARC-145 cells (Fei *et al*. 2011), floated and adherent cells were pelleted and washed in cold PBS and lysed with a cell extraction buffer (Invitrogen, USA) and 1 mM PMSF protease inhibitor (Thermo Fisher Scientific, USA). The lysates were centrifuged at 13,000 rpm for 10 mins at 4 °C. The protein concentration of cell extract supernatants was determined as the total protein (using the above method). The cell extract supernatants were then used to determine the concentration of monkey active caspase-3 levels (Wardi *et al*. 2014). The OD of this colored product was measured at 450 nm with an ELISA Reader (Thermo Fisher Scientific, USA), and this OD was directly proportional to the concentration of monkey active caspase-3 present in the sample. The results (ng/mg protein) were represented as monkey

active caspase-3 levels (ng) per protein concentration of cell extract supernatants (mg).

Determination of mouse anti-rcPAP polyclonal antibodies: The purified rcPAP (500 µg/ml) were submitted and the mouse polyclonal antibody against rcPAP was produced by ABGENEX Co. LTD (India). The immune-reactivity between the rcPAP and its mouse polyclonal antibodies was confirmed using western blot analysis, ELISA technique and IFA test (Guo *et al*. 2015).

Results

Cloning, expression and purification of rcPAP: We cloned the dsRBD of porcine PKR gene and CARD domain of porcine Apaf-1 genes from US strain PRRS virus-infected PAMs and constructed the prokaryotic expression plasmid of pET-P-A via LIC and pQE32-P-A, which was confirmed to be identical with GenBank data (No. KP729189 and No. KP729186) via DNA sequencing. Five models of the rcPAP were computationally generated using the I-TASSER algorithm with C-scores ranging from -4.27 to -4.52 (Fig. 1C and Table 4). Model 1 with a C-score of -4.27 was used for all analyses described (Fig. 1C). The rcPAP have 13 α-helices and 7 β-strands: α-α-α-β-β-β-α-α-β-β-β-α-α-α-α-α-α-α. Three dimensions of the dsRBD of porcine PKR protein which have 4 α-helices and 6 β-strands as shown: α-β-β-β-α-α-β-β-β-α with C-score 0.69. In addition, the CARD domain of porcine Apaf-1 protein has 6 α-helices with C-score 0.93. These results indicate that the rcPAP three-dimension have more 3 α-helices (one from plasmid, the second from TAT domain of HIV and the other from linker between the dsRBD and CARD domain, respectively) and one β-strand when compared with each of the dsRBD of porcine PKR protein and CARD domain of porcine Apaf-1 protein. In this study, the closest structural matches (TM-score = 0.82) of the dsRBD of porcine PKR protein and the CARD domain of porcine Apaf-1 (TM-score = 0.975) protein were human PKR (1QU6A) and human Apaf-1 (1Z6TB) proteins, respectively.

The recombinant proteins were expressed in *E. coli* upon IPTG induction. His-tagged rcPAP showed a band at approximately 35 kDa in the soluble fraction and reacted with the mouse anti-His monoclonal antibodies using the western blot technique. At low temperature, the expression levels of pQE32-P-A and pET-P-A plasmids were increased to 9.1 % and 22.7 %, respectively (Table 3). The rcPAP produced from the pET-P-A plasmids showed a higher expression level than that of the pQE32 plasmid and was chosen for further study. With the solubility of recombinant proteins, we observed that at high temperatures (30 and 37 °C), the solubility level showed less solubility (8.98 % and 3.1 %, respectively) than that at low temperatures (11.7 % at 18 °C and 19.8 % at 25 ˚C) (Fig. 2A-B and Table 5). We optimized the expression conditions of His-tagged rcPAP including the OD_{600} nm value 0.6, 0.75 mM of IPTG concentration and induction time at 18 h under an optimal temperature of 25 °C, respectively.

The soluble target proteins were purified under native conditions with a HiTrap chelating affinity column and eluted with a buffer containing 100-1,000 mM imidazole. Upon SDS-PAGE and western blot analysis this resulted in a molecular weight of 35 kDa when elution was from the column (Fig. 2C-D). The over expression of rcPAP was eluted at 400 mM of imidazole, 500 mM and 1,000 mM of imidazole. We also observed the rcPAP yields after a large amount of culture from different eluted fractions as shown (Table 6) and the highest amount of yield was at Elution 3 (14.21 mg per liter of bacterial culture). The recovery yields of the rcPAP approached 55.21 % (12.32 / 22.31 x 100 %) from 84.83 % (22.31 / 26.31 x 100 %) of the eluted proteins. The protein yield was estimated to be 12.32 mg/l on the Bradford assay.

Cell viability: The rcPAP in this study (40 µg/mL to 80 µg/mL) showed no cytotoxicity on Marc-145 cells (100 % of cell viability) at 48 h using either MTT or Trypan blue assays (Fig. 3). However, at a concentration of 120 µg/m, the rcPAP showed cytotoxicity and reduced 1.5 ± 0.28 % of cell viability upon MTT assay and 4.3 ± 0.09 % of cell viability upon Trypan blue assay.

Table 3 Expression levels of rcPAP at different-induction temperatures

Plasmids	Expression level (%)			
	18 °C	25 °C	30 °C	37 °C
pET-His6-TEV-LIC	9.3	22.7	16.7	19.5
pQE32	6.4	9.1	8.2	8.1

Table 4 The 3D structural prediction of rcPAP based on the deduced amino acid sequences using the I-TASSER method

Items	α-helices	β-strands	C-score
rcPAP model 1	13	7	-4.27
rcPAP model 2	13	7	-4.5
rcPAP model 3	13	7	-4.35
rcPAP model 4	13	7	-4.45
rcPAP model 5	13	7	-4.52
dsRBD of porcine PKR	4	6	0.69
CARD domain of porcine Apaf-1	6	0	0.93

Table 5 Solubility of rcPAP produced from the pET-His6-TEV-LIC plasmid at different induction temperatures

Items	Solubility level (%)			
	18 °C	25 °C	30 °C	37 °C
Soluble fraction	11.7	19.8	8.98	3.1
Pellet	9.02	17.2	15.5	14.7

Table 6 Concentrations (mg/L) of the rcPAP fractions

Fractions	Yields of rcPAP (mg/l)
Soluble	26.31
Flow through	0.07
Elution 1	1.63
Elution 2	4.73
Elution 3	14.21
Elution 4	1.13
Elution 5	0.61
Dialyzed rcPAP	12.32

Apoptotic induction on MARC-145 cells in the absence or presence of PRRS virus: We performed the apoptotic induction via monkey active caspase-3 ELISA assay to examine the bioactivity of rcPAP combined with PRRS virus-infected MARC-145 cells during early infection. As shown in Fig. 4, treatment with purified rcPAP (0, 2, 5, 10, 20, 40, 80 and 160 µg/mL) attenuated cell death and released levels of monkey active caspase-3 from the MARC-145 cells infected with PRRS virus in a concentration-dependent manner at 48 hpi ($P < 0.05$). The highest monkey active caspase-3 levels in the rcPAP at a dose of 80 µg/ml were 17.9 fold (9.150 ± 0.008 vs 0.510 ± 0.003 (ng/mg protein)), compared with the uninfected control. This finding confirmed that the purified protein markedly induced apoptosis in MARC-145 cells infected with PRRS virus.

Characterization of the mouse polyclonal antibodies: The specific mouse polyclonal antibodies greatly reacted with the purified rcPAP and showed a band at 35 kDa using western blot analysis (Fig. 5). Moreover, the mouse polyclonal antibodies showed a binding reactivity with the rcPAP in dilution manner when coating ELISA plates with 1.5 µg to 100 µg per well. A dilution of 10 showed OD_{450} values higher than that of a dilution of 50 (Fig. 6). The mouse polyclonal antibodies also showed specificity and reactivity with the rcPAP upon IFA test (Figs. 7A-B-C) by detection of the rcPAP which was delivered into the cytoplasm of MARC-145 cells. The results demonstrate that the purified rcPAP from E. coli had an appropriate function.

Discussion

Infection with swine virus such as PRRSV remains a significant pig health burden worldwide (Pileri and Mateu 2016). Currently, there is no effective prevention i.e. vaccines or preventive strategy to manage the PRRSV outbreak in the pig industry (Guo *et al.*, 2015). We have envisioned the development of alternate antiviral molecules with no infectious genetic material such as the swine recombinant DRACO proteins. This study relates to recombinant chimeric proteins with cell-targeting specificity and apoptosis-inducing activities. In particular, the chimeric protein

rcPAP specifically may target PKR-expressing cells and Apaf-1 induces cell-specific apoptosis. The rcPAP may be generated between any molecule that binds a specific viral infected cell type and an apoptosis-inducing protein as it allows this recombinant protein to control the viral infected cells and reduce the severity of the PRRSV outbreak.

To our knowledge, this is the first study that has attempted to construct the N-terminal of His6X with the dsRBD of porcine PKR gene and CARD domain of porcine Apaf-1 genes from US strain PRRS virus-infected PAMs. Herein, the composition of the synthetic peptides and the structure of rcPAP was analyzed and explored based on computational modeling using I-TASSER (Iterative Threading Assembly Refinement). The three dimension of the dsRBD of porcine PKR protein and CARD domain of porcine Apaf-1 protein clearly showed the significant modeling accuracy with the C-scores ranging from -4.27 to -4.52 (value of -1.5 as a cutoff for confidence in models) (Roy *et al*., 2010). Interestingly, the TM-score of both recombinant proteins was matched in the first I-TASSER model which aligned in the PDB library, possibly reflecting the identity in structural features of human origin.

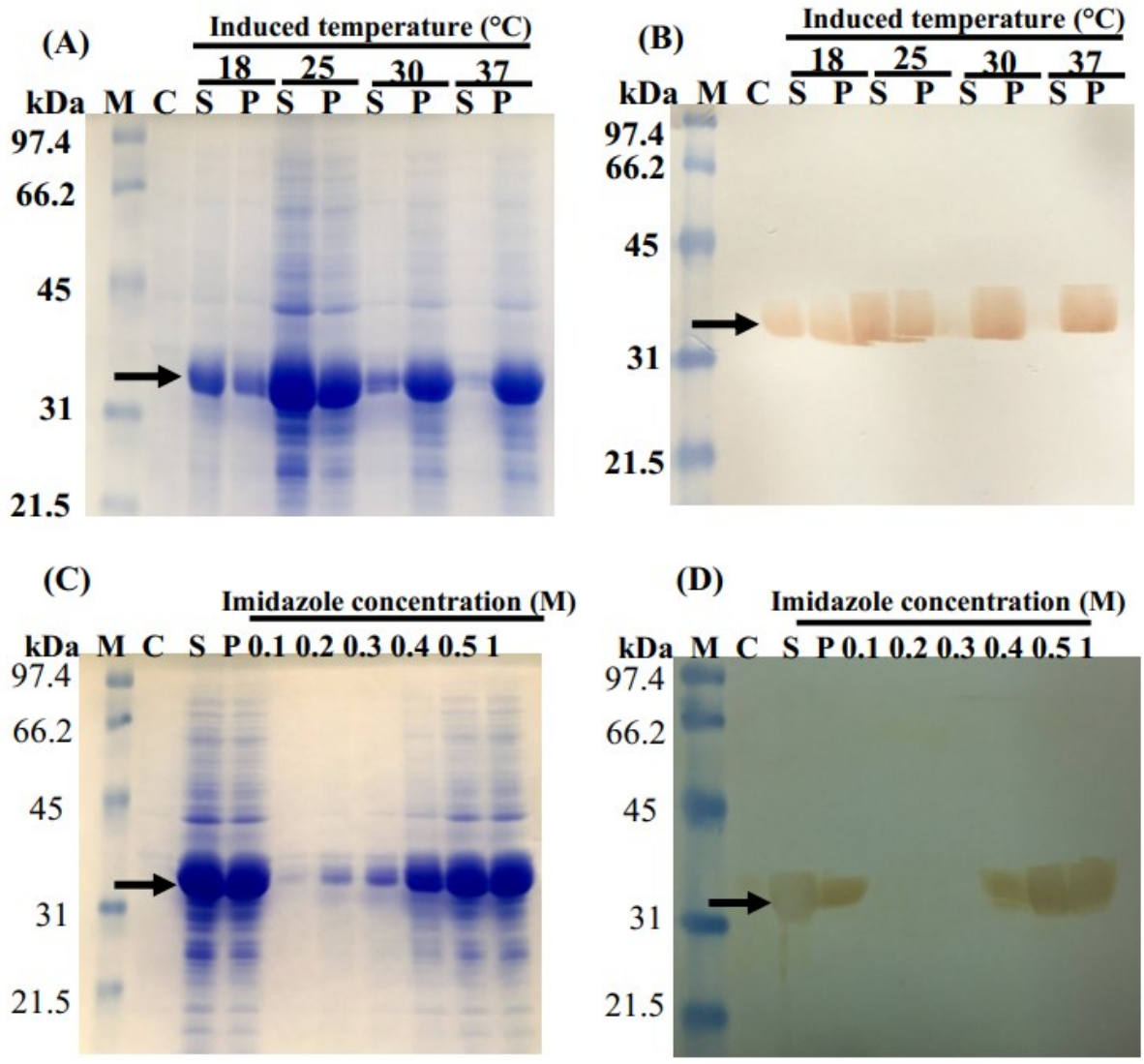

Figure 2 The Solubility and purification of rcPAP. Solubility test from the pET-His6-TEV-LIC plasmid was analyzed by 12.5 % SDS-PAGE (A) and by Western blot with mouse anti-His monoclonal antibodies (B). Purification of rcPAP was examined by 12.5 % SDS-PAGE (C) and western blot using mouse anti-His monoclonal antibodies (D). M, Protein markers (kDa); C, total cell protein before IPTG induction as a negative control; P, pellet fraction after cell sonication; S, soluble supernatant after cell sonication. lane 0.1, eluted with 100 mM imidazole; lane 0.2, eluted with 200 mM imidazole; lane 0.3, eluted with 300 mM imidazole, lane 0.4, eluted with 400 mM imidazole, lane 0.5, eluted with 500 mM imidazole, lane 1, eluted with 1,000 mM imidazole. Protein markers (BioRad) on the gels are indicated in kDa.

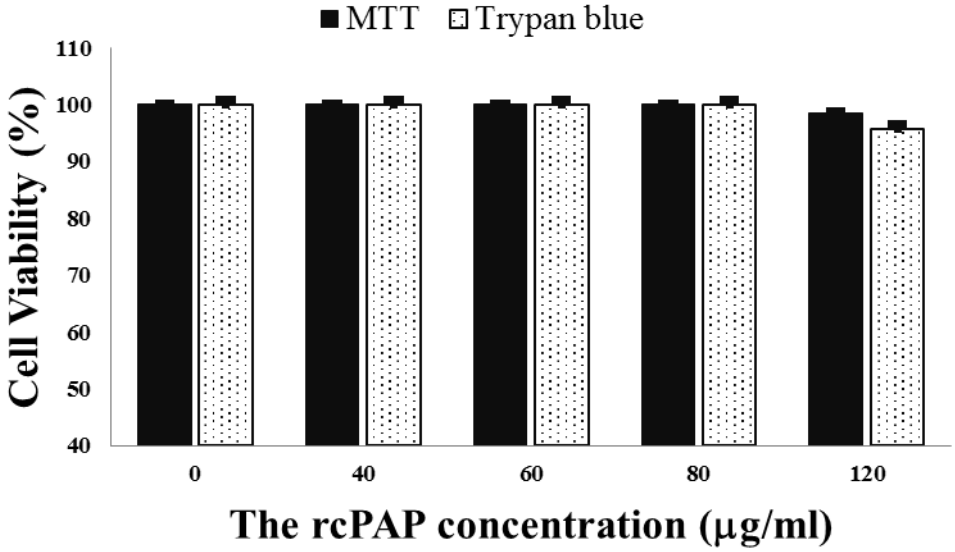

Figure 3 The cytotoxicity of the rcPAP in MARC-145 cells was measured using MTT and Trypan blue assay. Data is shown as mean ± SD of six independent experiments. Bars represent the standard deviation.

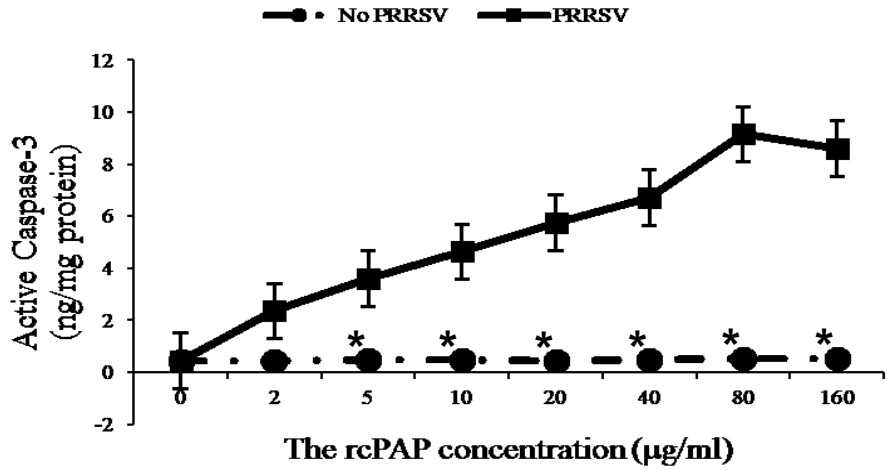

Figure 4 The monkey active caspase-3 levels in MARC-145 culture cells were measured via ELISA technique and the protein concentration measured. Data is shown as mean ± SD of six independent experiments. Bars represent the standard deviation. The $P < 0.05$ (*).

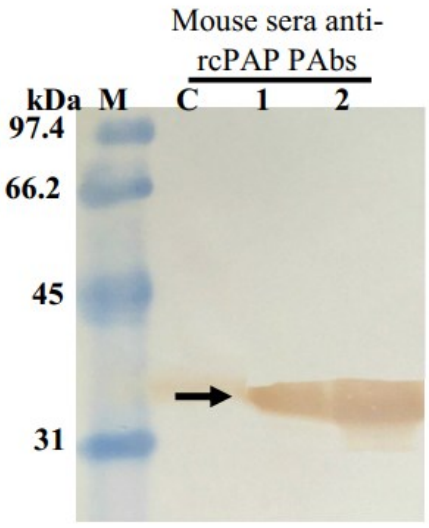

Figure 5 The reactivity of the mouse anti-rcPAP polyclonal antibodies against the rcPAP (80 µg/ml) using western blot analysis. M, protein markers kDa; C, total cell protein before IPTG induction as a negative control; 1, 5 fold dilutions sera anti-rcPAP PAbs; 2, 2 fold dilutions of sera anti-rcPAP PAbs. Protein markers (BioRad) on the gels are indicated in kDa.

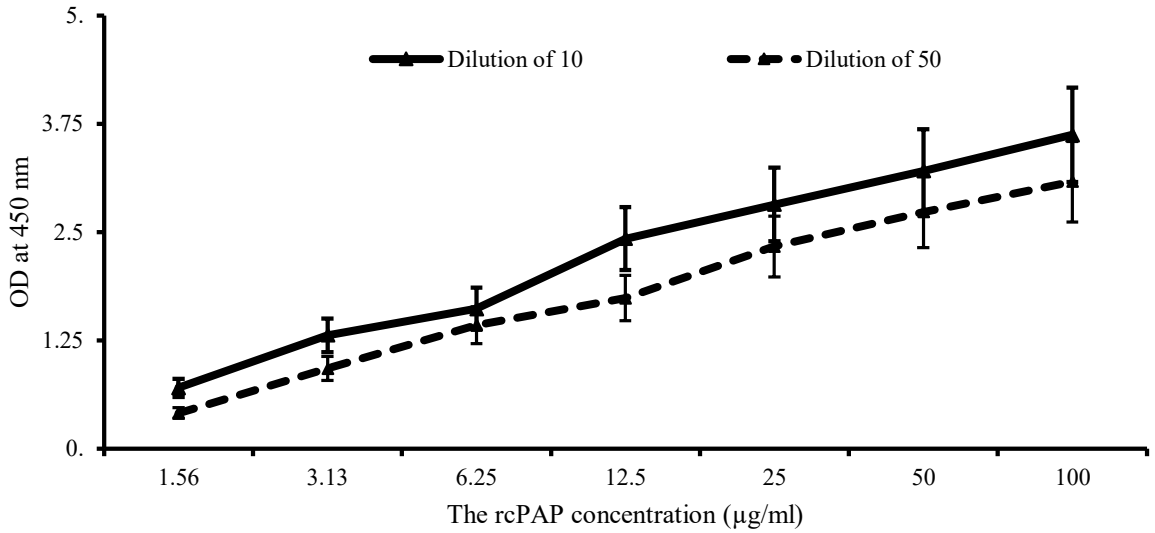

Figure 6 The mouse anti-rcPAP polyclonal antibodies were characterized using indirect ELISA. The OD values represent the average of two independent experiments that were performed in six replicates. The standard deviations are indicated by error bars.

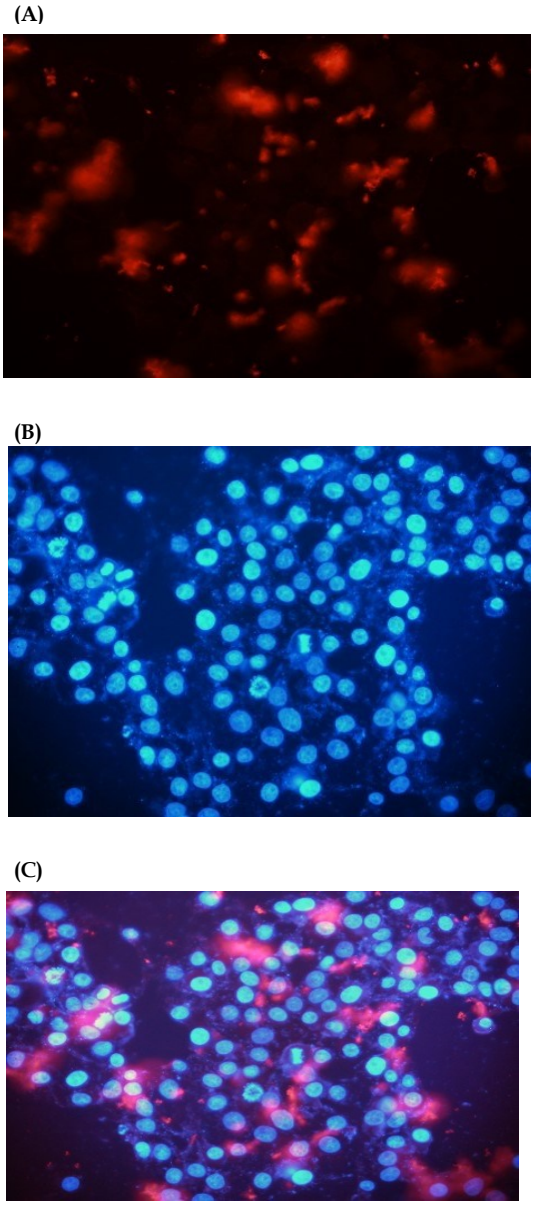

Figure 7 Characterization of the mouse anti-rcPAP polyclonal antibodies with IFA technique on MARC-145 cells. (A) the rcPAP are displayed in red. (B) the cell nuclei are shown in blue. (C) are merged.

We generated recombinant DNA molecules that direct the expression of this chimeric protein in appropriate *E coli* and undertook the expression of rcPAP between two bacterial expression plasmids including the pET-His6-TEV-LIC (pET-P-A) and the pQE32 (pQE32-P-A) plasmids. There was an approximately 22.7/9.1 fold increase in expression levels of the chimeric construct pET-P-A compared to the pQE32-P-A construct as assessed by ImageJ image analysis (Nguyen *et al*. 2014). It is believed that the poly-histidine-tag did not interfere with the expression levels of our recombinant protein and the pET-P-A plasmid produced the rcPAP with higher production efficiency than the pQE32-P-A, suggesting that pET-P-A is an appropriate expression vector. Numerous studies have shown that this discrepancy may occur due to some differences in replicon, promoter and host cells between the two plasmids. The pET plasmids with the pMB1 origin (15-60 copies per cell) showed higher copies per cell compared to the pQE plasmids (15-20 copies per cell) (Rosano and Ceccarelli 2014). This implies that high plasmid dosage, equivalent to having many expression units reside in the cell, may produce more recombinant protein yields (Boustanshenas *et al*. 2013). Consistent with the study results of Suryanarayana *et al*., (2016), the pET plasmid showed that the yield of recombinant proteins was twice as high as the pQE plasmid. Based on conditions of the protein expression and the yield of soluble protein, production can be optimized by varying induction temperatures, inducer concentrations and OD_{600} nm (Gupta and Shukla 2015). We studied the possibility of increasing the opportunity for high-yield expression and solubility of rcPAP at 18-37 °C, which consists of cell density, IPTG concentration, and induction time. 25 °C is better to achieve higher rcAPAP soluble protein. In particular, protein expression at a low temperature often significantly improves the solubility of recombinant proteins (Gupta and Shukla 2015). In this study, the rcPAP produced from the pET-P-A plasmid with induction at lower temperatures (18–25 °C) showed a high amount of the soluble rcPAP without the modification of the protein extraction method and this indicated that there is a decrease in the formation of inclusion bodies (Rosano and Ceccarelli 2014). In general, the culture of *E. coli* at low temperature helps to make the expression of more soluble foreign proteins possible(Sørensen and Mortensen 2005, de Groot and Ventura 2006). Moreover, a high concentration of IPTG increases toxicity in *E. coli* (Onodera *et al*. 1996) and inhibits cell growth. We have results that increasing the OD_{600} nm of a culture more than 0.6, an induction time longer than 18 h and increasing IPTG concentrations more than 0.75 mM did not significantly increase the expression yield of the recombinant proteins (data not shown). We can conclude that the most suitable conditions for rcPAP expression were induction at 25 °C for 18 h with the addition of 0.75 mM IPTG when the OD_{600} nm of the pET-P-A culture reached 0.6. After parameters opimisation, a high yield of rcPAP protein was achieved in soluble form at a low-induction temperature and could be purified under native conditions. In practice, the soluble protein can reduce the process of recovering the insoluble protein, the time and potential cost necessary for purification and also reduce the removal of the cross-flow filtration, denaturing and refolding steps (Kim *et al*. 2013). In this study, we chose to use a HiTrap Chelating HP column charged with Ni^{2+} for purification of the His6X-rcPAP (Heijbel, 2003 and Kim *et al*., 2013) and also the presence of the N-terminal-residue polyhistidine sequence did not affect yields. The rcPAP protein can be purified in one-step using affinity column and used directly without further purification. While the present expression system produces adequate amounts of protein for in vitro characterization, the production of large amounts of protein for animal studies will require an alternative expression host such as yeast or mammalian cells with naturally produced proteins.

To study its immunogenicity properties, we produced the specific polyclonal antibodies in BALB/c mice and characterized mouse antibodies using western blotting, the IFA test and developed indirect ELISA analysis. The results from western blotting and the developed indirect ELISA indicate that mouse antibodies contained specific antibodies against rcPAP and had a specific binding activity. Notably, polyclonal antibody can detect the rcPAP protein in the cytoplasm of MARC-145 cells by using IFA technique, suggesting that mouse antibodies may maintain their natural immune function. Therefore, the generating antibodies can be used for binding to epitopes of rcPAP to facilitate their further purification and will be useful for the immunoassay for rcPAP.

The attenuating effects of rcPAP on PRRS virus-infected cells are of interest with the PKR detecting and Apaf-1 inducing apoptotic property attributed to this antiviral molecule by reducing the viral infection. Previous studies have reported that PRRS virus stimulates anti-apoptotic pathways in MARC-145 cells and PAMs in early infection and PRRS virus-infected cells also die from apoptosis in late infection (Costers *et al*., 2008). Apoptosis is considered to be an important host-defense mechanism that interrupts viral replication and eliminates virus-infected cells (Koyama *et al*., 2008). In the recombinant chimeric protein model, with viral-infected cells, two or more dsRNA binding domains of porcine PKR were cross-linked on the same-viral dsRNA and the effector domain would then activate caspase 9 and trigger apoptosis (Elmore, 2007; Rider *et al*., 2011). This study also indicated that the concentration of rcPAP at 40, 60 and 80 µg/mL was not toxic to Marc-145 cells by using MTT assay and Trypan blue assay. The Human DRACO molecule produced from bacteria (5 to 20 µg/mL) also reported no toxicity in 11 studied cell lines (Rider *et al*., 2011). However, observation of cytotoxicity of rcPAP on swine cell lines and primary cells origin and the reduction of bacterial toxin using antitoxin absorbent column are needed to be further studied. We demonstrated that the rcPAP can penetrate and bind into the cytoplasm of MARC-145 cells detected using IFA technique (Fig. 7). In that connection, the HIV-TAT domain of this recombinant protein successfully delivered the rcPAP through MARC-145 cell membrane and the 6x-histidine-tag did not interfere with the process of penetration (Vo and Nuntaprasert 2015). In addition, the HIV-TAT domain has been used to deliver human DRACO protein getting to about 11 human cell lines and to the mouse

cells as well (Rider *et al*., 2011). In the swine model, this domain also showed the potential delivery of the PRRS virus nucleocapsid and the matrix protein into the PK-15 cell line, dendritic cells and peripheral blood mononuclear cells (Jeong *et al*., 2010). For dsRNA detection properties of rcPAP, the dsRBD of PKR protein were selected to recognize and bind to viral dsRNA in virus-infected cells (Guo *et al*., 2015; Rider *et al*., 2011). Considering the structural similarities, porcine PKR protein had a similar function to other mammalian PKR protein (Asano *et al*., 2004). We confirmed that the dsRBD of the porcine PKR gene in rcPAP protein can recognize dsRNA in PRRS virus-infected monkey cells. For effector domain properties of rcPAP, we selected and used the CARD domain from porcine Apaf-1 gene for activation of initiator apoptotic pathway to induce apoptosis in virus-infected cells (Rider *et al*., 2011). In order to examine this apoptotic effect of rcPAP on PRRS virus-infected MARC-145 cells by evaluating monkey active caspase-3 levels using commercial ELISA assay was employed. We clearly demonstrated that rcPAP (80 μg/mL) significantly induced apoptotic protein by increasing the monkey active caspase-3 levels by 17.9 fold in PRRS virus-infected MARC-145 cells at 48 hpi (P <0.05) compared with the uninfected control. In agreement with the results from Guo *et al*.. (Guo *et al*.. 2015) our rcPAP also induced apoptosis in PRRS virus- infected MARC-145 cells. In our study, we also found that rcPAP induced apoptosis in US-PRRS virus-infected MARC-145 cells. The result shows that our rcPAP can induce apoptosis in PRRS virus-infected cells. The enhancing effect of rcPAP on apoptosis production may be explained by the activation of CARD domain of Apaf-1 through apoptosis in virus-infected cells (Guo *et al*., 2015; Rider *et al*., 2011) and rcPAP could induce apoptosis on PRRS virus-infected MARC-145 cells via activation of caspase 9 (an initiator caspase in intrinsic apoptotic pathway) (Elmore, 2007). Once activated, active caspase 9 activates caspase 3 (the key protease activated during early apoptosis as apoptotic marker) (Elmore, 2007). Interestingly, the rcPAP did not induce apoptosis on normal cells (viral dsRNA are not present) because of the very low detection of monkey active caspase-3 levels on uninfected MARC-145 cells.

We can infer that three parts in our molecules have successfully done their work on virus-infected cells and this rcPAP produced in *E. coli* can induce apoptosis inducing protein caused programmed cell death in mammalian cells (monkey cells). Based on these finding, we can imply that the rcPAP produced in this study has high bioactivity for further investigation *in vitro* and *in vivo*.

In summary, we successfully cloned, expressed and purified the soluble rcPAP in *E. coli*. under native conditions. Our approach allowed the efficient optimization of the expression of recombinant proteins. The purified rcPAP exhibited apoptosis activity in MARC145 cells. This active recombinant protein may be useful for targeting swine virus infection such as PRRSV regarding rcPAP as antiviral molecules which will be useful for further study to control swine-viral infection.

Acknowledgements

This work was supported by the Chulalongkorn University Research Experience Scholarship for Graduate Students.

References

Asano, A., Y. Kon and T. Agui (2004). The mRNA regulation of porcine double-stranded RNA activated protein kinase gene. J Vet Med Sci. 66: 1523-1528.

Billack, B., V. Radkar and C. Adiabouah (2008). In vitro evaluation of the cytotoxic and antiproliferative properties of resveratrol and several of its analogs. Cell Mol Biol Lett 13: 553-569.

Boustanshenas, B., B. Bakhshi, M. Ghorbani and D. Norouzian (2013). Comparison of two recombinant systems for expression of cholera toxin B sununit from Vibrio cholerae. Indian J Med Microbiol. 31: 10-14.

Charerntantanakul, W. (2012). Porcine reproductive and respiratory syndrome virus vaccines: Immunogenicity, efficacy and safety aspects. World J Virol. 1: 23-30.

Cui, J., J. Xie, M. Gao, H. Zhou, Y. Chen, T. Cui, X. Bai, H. Wang and G. Zhang (2015). Inhibitory effects of lithium chloride on replication of type II porcine reproductive and respiratory syndrome virus in vitro. Antiviral Therapy 20: 565-572.

de Groot, N. S. and S. Ventura (2006). Effect of temperature on protein quality in bacterial inclusion bodies. FEBS Lett. 580: 6471-6476.

Ding, X., F. Xu, H. Chen, R. B. Tesh and S. Xiao (2005). Apoptosis of Hepatocytes Caused by Punta Toro Virus (Bunyaviridae: Phlebovirus) and Its Implication for Phlebovirus Pathogenesis. Am J Pathol 167: 1043-1049.

Fei, Z., Y. Liu, Z. Yan, D. Fan, A. Alexander and J. Yang (2011). Targeting viral dsRNA for antiviral prophylaxis. FASEB J. 25: 1-8.

Gao, L., W. Zhang, Y. Sun, Q. Yang, J. Ren, J. Liu, H. Wang and W. Feng (2013). Cryptoporus volvatus Extract Inhibits Porcine Reproductive and Respiratory Syndrome Virus (PRRSV) In Vitro and In Vivo. PLoS ONE 8: 1-10.

Gump, J. M. and S. F. Dowdy (2007). TAT transduction: the molecular mechanism and therapeutic prospects. Trends Mol Med. 13: 443-448.

Guo, C., L. Chen, D. Mo, Y. Chen and X. Liu (2015). DRACO inhibits porcine reproductive and respiratory syndrome virus replication in vitro. Arch Virol. 160: 1-9.

Gupta, S. K. and P. Shukla (2015). Advanced technologies for improved expression of recombinant proteins in bacteria: perspectives and applications. Crit Rev Biotechnol. 36: 1-10.

Kim, M., H. S. Park, K. H. Seo, H. Yang, S. Kim and J. Choi (2013). Complete Solubilization and Purification of Recombinant Human Growth Hormone Produced in Escherichia coli. PLoS ONE 8: 0056168.

Le, V. P., D. G. Jeong, S. W. Yoon, H. M. Kwon, T. B. N. Trinh, T. L. Nguyen, T. T. N. Bui, J. Oh, J. B. Kim, K. M. Cheong, T. N. Van, E. Bae, T. T. H. Vu, M. Yeom, W. Na and D. Song (2019). Outbreak of African

Swine Fever, Vietnam, 2019. Emerg Infect Dis 25(7): 1433-1435.

Li, Y., X. Wang, K. Bo, X. Wang, B. Tang, B. Yang, W. Jiang and P. Jiang (2007). Emergence of a highly pathogenic porcine reproductive and respiratory syndrome virus in the Mid-Eastern region of China. Vet J. 174: 577-584.

MacroLab, Q. (2014). LIC Expression Vectors: A Laboratory Manual. 8: 1-31.

Nguyen, M. T., B. Koo, T. T. T. Vu, J. Song, S. Chong, B. Jeong, H. Ryu, S. Moh and H. Choe (2014). Prokaryotic Soluble Overexpression and Purification of Bioactive Human Growth Hormone by Fusion to Thioredoxin, Maltose Binding Protein, and Protein Disulfide Isomerase. PLoS ONE 9: 0089038.

Onodera, O., A. D. Roses, S. Tsuji, J. M. Vance, W. J. Strittmatter and J. R. Burke (1996). Toxicity of expanded polyglutamine-domain proteins in Escherichia coli. FEBS Lett. 399: 135-139.

Pileri, E. and E. Mateu (2016). Review on the transmission of porcine reproductive and respiratory syndrome virus between pigs and farms and impact on vaccination. Vet. Res. 47(108).

Pozzo, F. D. and E. Thiry (2014). Antiviral chemotherapy in veterinary medicine: current applications and perspectives. Rev Sci Tech Off Int Epiz. 33: 1-27.

Rider, T. H., C. E. Zook, T. L. Boettcher, S. T. Wick, J. S. Pancoast and B. D. Zusman (2011). Broad-Spectrum Antiviral Therapeutics. PLoS ONE 6: 1-15.

Riedl, S. J., W. Li, Y. Chao, R. Schwarzenbacher and Y. Shi (2005). Structure of the apoptotic protease-activating factor 1 bound to ADP. Nature 434: 926-933.

Rosano, G. L. and E. A. Ceccarelli (2014). Recombinant protein expression in Escherichiacoli: advance sand challenges. Front Microbiol. 5: 1-17.

Roy, A., A. Kucukural and Y. Zhang (2010). I-TASSER: a unified platform for automated protein structure and function prediction. Nat Protoc. 5: 725-738.

Sørensen, H. P. and K. K. Mortensen (2005). Soluble expression of recombinant proteins in the cytoplasm of Escherichia coli. Microb Cell Fact. 4: 1-8.

Uma, S., J. P. Kelly and S. K. Rajasekaran (2008). An investigation of the value of the Tetrahymena pyriformis as a test organism for assessing the acute toxicity of antidepressants. Biomed Res 19: 37-40.

Valiyari, S., B. Baradaran, A. Delazar, A. Pasdaran and F. Zare (2012). Dichloromethane and Methanol Extracts of Scrophularia oxysepala Induces Apoptosis in MCF-7 Human Breast Cancer Cells. Adv Pharm Bull 2: 223-231.

Vo, P. V. A. T. and A. Nuntaprasert (2015). Production of recombinant chimeric swine PKR-Apaf1 proteins in E.coli from porcine alveolar macrophages (PAMs). Proceedings of the 7th Asian Pig Veterinary Society Congress. Manila, Philippine: O76.

Wardi, L., N. Alaaeddine, I. Raad, R. Sarkis, R. Serhal, C. Khalil and G. Hilal (2014). Glucose restriction decreases telomerase activity and enhances its inhibitor response on breast cancer cells: possible extra-telomerase role of BIBR 1532. Cancer Cell International 60: 1-14.